



Short communication

A facile one-pot synthesis of Ag₂Te nanoparticles and the fabrication of nanocomposites for the removal of chromium (VI) in wastewater

O. Sentse^a, T. Xaba^{a,*}, N.D. Shooto^a, V.E Pakade^b, W. Omwoyo^c^a Department of Biotechnology & Chemistry, Vaal University of Technology, Private Bag X 021, Vanderbijlpark, South Africa^b Department of Chemistry, College of Science and Engineering and Technology, Florida Science Campus, University of South Africa, Roodepoort, Johannesburg, 1710, South Africa^c Maasai Mara University, P.O. Box 861-20500 Narok, Kenya

ARTICLE INFO

Keywords:

Silver tellerium
PVA
Chitosan
Nanocomposites
chromium (VI) ions
Adsorption

ABSTRACT

The sol-gel method has been used successfully for the preparation of crystalline PVA-Ag₂Te nanoparticles at room temperature using water as a solvent, PVA as a capping agent, sodium borohydride as a reducing agent, tellerium, and silver nitrate as a source of silver. The synthesized PVA-Ag₂Te were then incorporated with chitosan to form the nanocomposites for the removal of Cr(VI) ions from wastewater. A blue shift in the wavelength was observed with an energy band gap between 2.76 eV and 2.82 eV when the PVA was added into the nanoparticles. The morphology and structural studies of the particles were carried out using transmission electron microscopy (TEM) and powder-X-ray diffraction (XRD). The XRD patterns of the Ag₂Te projected a pure monoclinic phase whereas TEM images showed agglomerated spherical shaped particles that were improved when the stabilizers was introduced into the nanomaterial with the average particle sized between 8.77 and 9.12 nm. The adsorption process was able to verify that the parameters such as pH, contact time, and initial concentration had a huge impact on water treatment processes. The essential parameters of Langmuir and Freundlich adsorption isotherms were successively utilized to analyze the adsorption mechanism. This was accomplished by combining the isotherms equation with mass conservation of solute before and after adsorption.

1. Introduction

The discharge of heavy metals into wastewater through industrial chemical processes and human activities has become a major issue to both aquatic and human lives [1]. Wastewater liberated from such processes usually contain toxic substances that can harm the environment. The high concentrations of harmful metals in our water systems may cause obstructions with biological treatment processes during sewage treatment [2]. Chromium is one of the heavy metal that is classified as a toxic pollutant that have harmful effects on human's life. The high level of chromium may cause damage and health complications such as liver damage and human kidney disorder [3]. Several methods have been applied for the removal of Cr(VI) from wastewater systems but among these techniques, adsorption has been considered as the most appropriate approach since it is more applicable and simple to accomplish [4].

Nanoparticles have been used recently to enhance the surface charge of the composites for wastewater treatment. Silver chalcogenides,

especially Ag₂Te, have been receiving remarkable attention lately due to their stimulating semiconducting properties. Capping molecules such as starch, polyethylene glycole, ploviny pyrrolidone etc are generally used in synthesis to prevent nanoparticle's aggregation as well as to control the structural characteristics of the nanoparticles [5].

The synthesis of Ag₂Te nanostructures is in demand as these nanostructures have enhanced properties as compared to their corresponding bulk counterparts for the development of new generation nano-devices [6]. Ag₂Te is well-known to show phase modification from the low-temperature monoclinic phase (β -Ag₂Te) to the high temperature face-centered cubic phase (α -Ag₂Te) at approximately 423 K [7]. The pure monoclinic phase Ag₂Te nanowires were prepared by a simple solvothermal method without a template and surfactant by Chang and coworkers [8] by adjusting the raw material ratios. The preparation of silver nanoparticles in a plasma-liquid system in the presence of PVA was reported by Skiba and co-workers. The influence of the basic parameters such as initial concentration, PVA concentration, and process duration on the formation of silver nanoparticles and their

* Corresponding author.

E-mail address: thokozanix@vut.ac.za (T. Xaba).<https://doi.org/10.1016/j.inoche.2023.111755>

Received 21 August 2023; Received in revised form 13 November 2023; Accepted 16 November 2023

Available online 23 November 2023

1387-7003/© 2023 Elsevier B.V. All rights reserved.

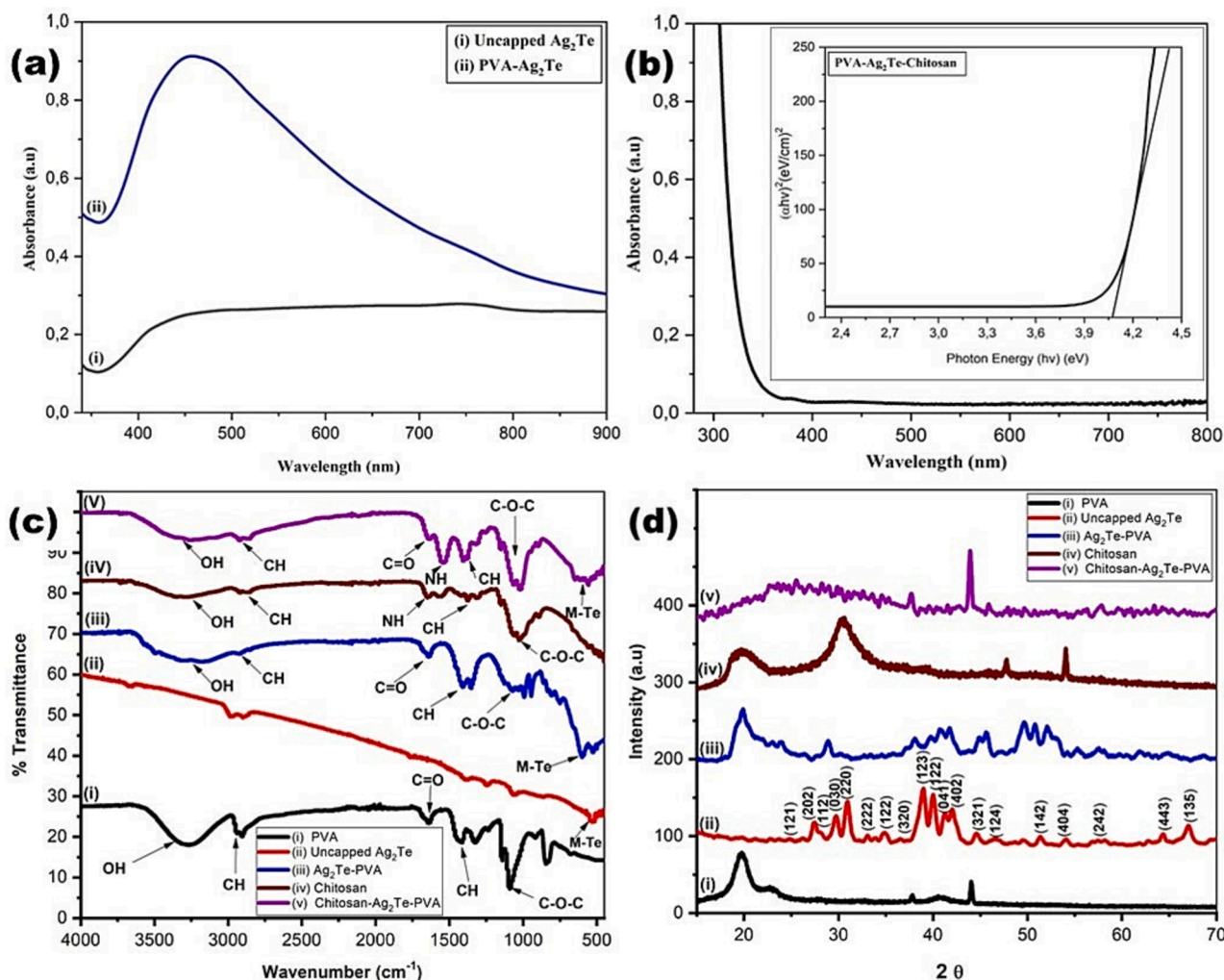


Fig. 1. UV-vis spectra of uncapped Ag₂Te, Ag₂Te-PVA nanoparticles (a), absorption spectrum & Tauc plot (b) of PVA-Ag₂Te-Chitosan, FTIR spectra (c) and XRD patterns of nanoparticles and nanocomposites (d).

characteristics were investigated [9]. Nawaz and colleagues used an eco-friendly method to prepare iron oxide nanoparticles/polyvinyl alcohol nanocomposite and their potential adsorption properties against designated heavy metals was conducted [10]. Recently, we have reported the green synthesis of ZnS nanoparticles and fabrication of ZnS-chitosan nanocomposites for the removal of Cr(VI) ion from wastewater [11].

For the first time, we report the effective removal of hexavalent chromium ions from wastewater samples using PVA-Ag₂Te-Chitosan nanocomposites prepared from PVA-Ag₂Te nanoparticles that were synthesized using the sol-gel which is regarded as simple and straight forward method. The pure chitosan solution was also used during the adsorption process to compare the percentage removal between pure chitosan and nanocomposites. The effects of parameters such as pH, contact time, and initial chromium ions concentrations on the performance of the adsorbents were investigated.

2. Experimental

2.1. Materials

Chitosan medium molecular weight, tellerium powder and polyvinyl alcohol (PVA) were bought from Sigma-Aldrich. Ammonium hydroxide, sodium hydroxide, potassium dichromate, sodium borohydride and silver nitrate were purchased from Merck Chemical Company (SA) and hydrochloric acid was purchased from GlassWorld (SA).

2.2. Synthesis of Ag₂Te-PVA nanoparticles

Exactly 1 mL solution of Ag₂NO₃ (0.011 mmol) was added into 0.5 % PVA (20.0 mL) in a one necked flask. The solution was stirred at room temperature for 10 minutes. The pH of the solution was then adjusted to a basic form with 0.1 M ammonium hydroxide solution. Exactly 1 mL of solution of Tellerium (0.032 mmol) prepared by dissolving powder tellerium in warm water for 12 hrs was added and the solution was further stirred for 20 hrs at room temperature. At the end of the reaction, a black precipitate of Ag₂Te-PVA was recovered. The black powdered product was washed three times with acetone, centrifuged and dried in an open air.

2.3. Preparation of PVA-Ag₂Te-Chitosan nanocomposites

About 3 mg of Ag₂Te-PVA nanoparticles was dispersed in 10.0 mL of deionized water and ultrasonicated for 30 min to dissolve the nanoparticles. The solution was then filtered and the filtrate was transferred into a 100 mL beaker that contained 50.0 mL of 1 % chitosan solution. The beaker was sealed with a foil and the mixture was ultra-sonicated for 4hr. About 5.0 mL of PVA-Ag₂Te-Chitosan nanocomposite was transferred into a petri dish. The dish with the product was allowed to evaporate inside the fume hood for 24 hrs to form PVA-Ag₂Te-Chitosan nanocomposite films. The remaining PVA-Ag₂Te-Chitosan polymer nanocomposite solution was kept for water treatment.

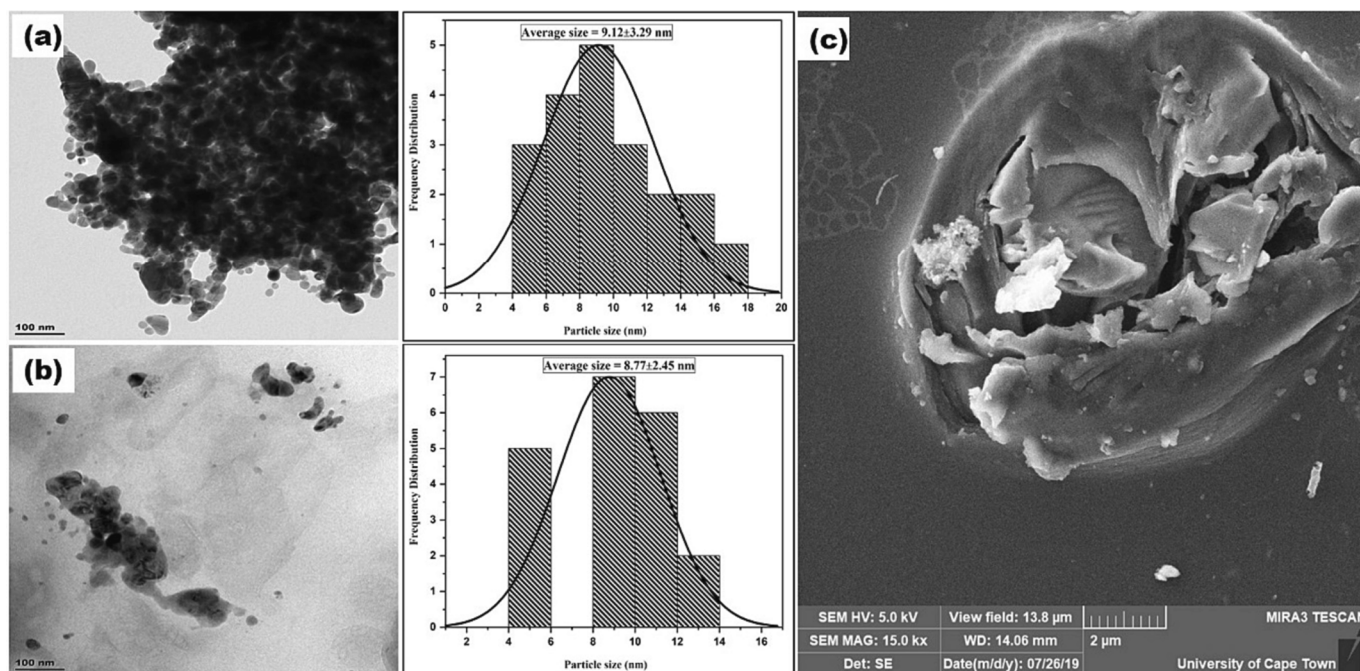


Fig. 2. TEM micrographs of uncapped Ag_2Te (a), Ag_2Te -PVA (b) together with it corresponding histograms and SEM image of PVA- Ag_2Te -Chitosan nano-composite (c).

2.4. Batch adsorption studies.

A 1000 ppm stock solution of heavy metal was prepared by dissolving 1.415 g of Cr(VI) salt in 500 mL of distilled water. Different concentrations ranging from 20 to 100 ppm were attained by dilution method from the stock solution. Exactly 20.0 mL of the ion metal solution was shaken at 250 rpm in a plastic bottle for each experiment. The pH of the solution was adjusted by adding 0.1 M NaOH or 1.0 M HCl to the preferred value. The thermostat shaker was used to carry out adsorption studies at room temperature at a speed rate of 250 rpm.

2.5. Characterization

UV-1800 Shimadzu spectrophotometer and Gilden Fluorescence were used to determine the optical properties of Ag_2Te nanoparticles and chitosan- Ag_2Te nanocomposite. X-ray diffraction patterns were collected on a Phillips X'Pert chemistry research diffractometer using secondary monochromated $\text{Cu K}\alpha$ radiation ($\lambda = 1.54060 \text{ \AA}$) at 40 Kv/30 mA. Transmission electron microscopy (TEM) was ran using a Tecnai F30 FEG TEM instrument at an accelerating voltage of 300 kV to collect the images of the nanoparticles. The FTIR measurements were attained at room temperature at a scan range between 400 and 4000 cm^{-1} . Adsorption analysis were obtained on the AA-7000 Shimadzu model coated GFA-7000 graphite furnace atomizer.

3. Results and discussion

3.1. Ag_2Te capped with PVA nanoparticles and PVA Ag_2Te -Chitosan nanocomposites

Fig. 1(a) shows absorption spectra of the uncapped Ag_2Te with absorption maxima at 450 nm. A broad peak in an absorption spectrum of PVA- Ag_2Te nanoparticles with absorption maxima at 440 nm was also observed. The results were blue shifted from their bulk material Ag_2Te which is at 673 nm. This signifies the quantum confinement [12]. Fig. 1 (b) shows the absorption spectrum of PVA- Ag_2Te -Chitosan which is located at 302 nm with a band gap energy of 4.02 (eV). Fig. 1(c) (i, ii & v) shows the FTIR spectra of Ag_2Te displayed a peak around 523 cm^{-1}

that was attributed to the metal telluride. In the FTIR of PVA- Ag_2Te , a broad peak at 3255 cm^{-1} was observed which corresponds to the O-H functional group of PVA indicating the presence of PVA in the Ag_2Te nanoparticles. It was also observed that when the capping molecule was introduced onto the nanoparticles, the functional groups of O-H, C-H, C-O-C, and C-O were slightly shifted. These observations confirmed the capping of PVA onto Ag_2Te .

The XRD pattern of PVA in Fig. 1 (d)(i) displayed a diffraction peak at $2\theta = 18.2^\circ$ that is associated with the polymorph of the PVA. The XRD patterns of uncapped Ag_2Te were indexed to a pure monoclinic phase, which is very close to the literature values (JCPDS No. 34-0142) [13]. The narrow sharp peaks denote that the Ag_2Te nanoparticles are well crystallized. The XRD pattern of the PVA- Ag_2Te nanoparticles showed similar diffraction peaks as the uncapped nanoparticles. The XRD pattern of chitosan showed two peaks at $2\theta = 20^\circ$ and 30° that were associated with the characteristics of the hydrated crystalline structure of chitosan [14]. Most of the peaks disappeared in the XRD pattern of PVA- Ag_2Te -Chitosan nanocomposite which is an indication that the incorporation of chitosan with PVA- Ag_2Te was successful.

The broadening of the XRD patterns of the synthesized Ag_2Te nanoparticles indicates the formation of small size particles. The average crystallite sizes were found using the Debye Scherrer formula (Eq. (1) [15,16]:

$$d = 0.9(\lambda)/\beta\cos\theta \quad (1)$$

where λ is wavelength (1.5418 \AA) and β is the full width half maximum (FWHM) of corresponding peaks. The calculated crystallite sizes of the synthesized Ag_2Te nanoparticles were between 6.20 and 6.01 nm for the uncapped Ag_2Te and PVA capped Ag_2Te which is very close to the TEM results obtained below.

Electron transmission microscopy (TEM) was used to investigate the sizes and the shapes of the uncapped and PVA capped Ag_2Te nanoparticles. TEM images of the synthesized nanoparticles in Fig. 2(a-b) shows the agglomerated particles. It was also noted that when PVA was introduced into the nanoparticles, a minor dispersity and little bit of closely packed nanoparticles was observed. SEM image in Fig. 2(c) of PVA- Ag_2Te -Chitosan projected morphology of the particles that is consisting of the abnormal, rough and irregular particle. The combination of

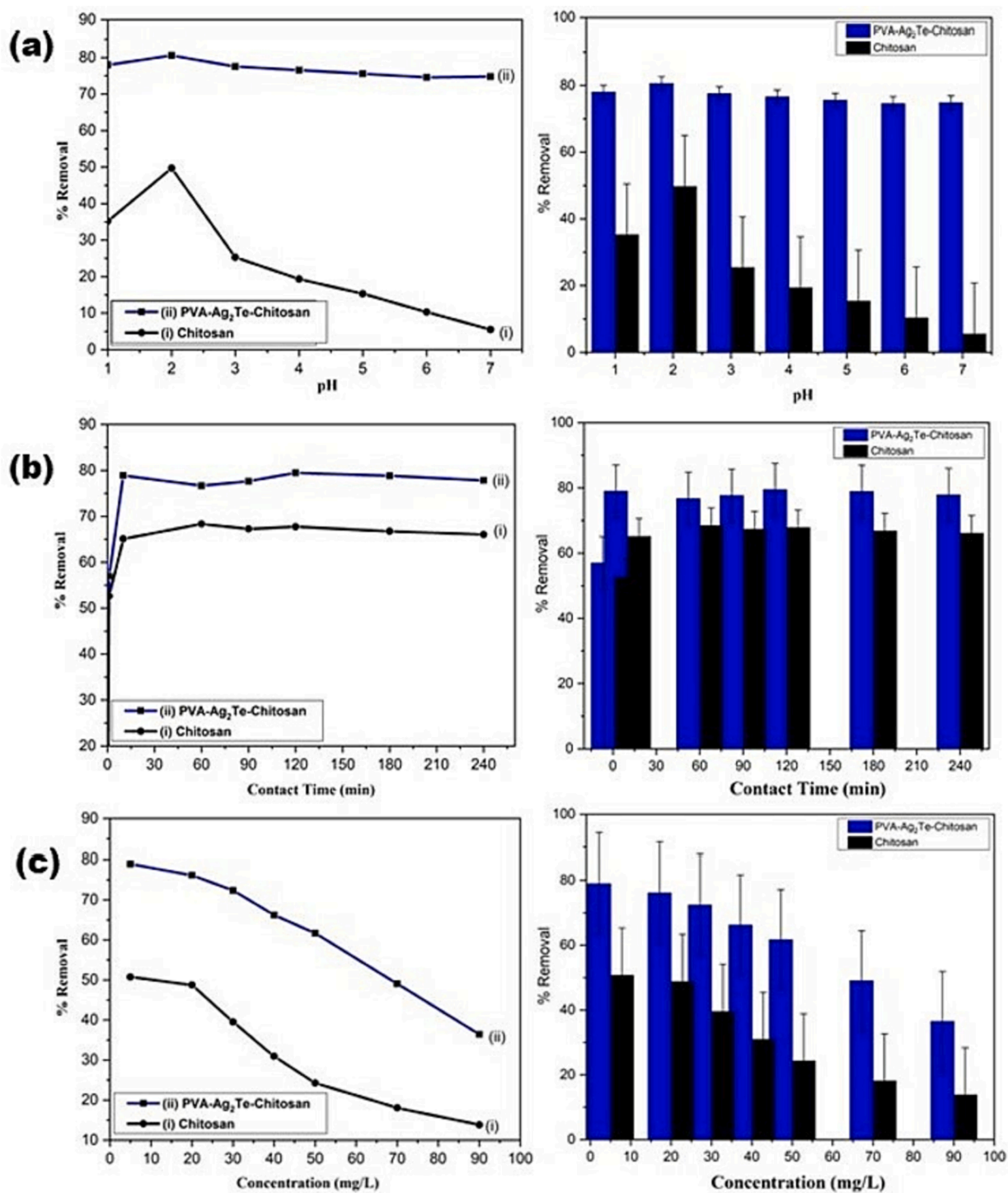


Fig. 3. Effect of pH (a), contact time (b) and initial concentration (c) on adsorption of Cr(VI) ions using Chitosan (i) and PVA-Ag₂Te-Chitosan (ii).

the capped nanoparticles and the chitosan appear to have linked to form interconnected clusters. This may suggest a proper adsorption abilities towards the Cr(VI).

3.2. Adsorption process

The amount of chromium (VI) removed was calculated from the following equation (2):

$$\%R = \frac{C_0 - C_f}{C_0} \times 100 \quad (2)$$

where: C_0 (mg/L) is the initial metal ion concentration and C_f (mg/L) is the final metal ion concentration in the solution.

Langmuir (Eq. (3)) and Freundlich (Eq. (4)) adsorption isotherm models were used for fitting equilibrium data to describe the sorption process [17].

$$\frac{C_e}{q_e} = \frac{1}{K_L q_m} + \frac{C_e}{q_m} \quad (3)$$

$$\ln q_e = \ln K_F + \frac{1}{n \ln C_e} \quad (4)$$

Table 1
Langmuir and Freundlich isotherms for the PVA-Ag₂Te-Chitosan.

Model	Parameter	PVA-Ag ₂ TeChitosan
Langmuir	q _{e(cal)} (mg/g)	97.087
	k _L (Lmg ⁻¹)	0.160
	R ²	0.978
	R _L	0.065
Freundlich	K _f (mg ⁻¹)	3.472
	N	2.155
	R ²	0.935
Experimental q _{e(exp)}	(mg/g)	89.852

3.2.1. Effect of pH, dosage, contact time, and initial concentration

The influence of solution pH on the adsorption of Cr(VI) was investigated by varying the pH from 2 to 10, while other parameters were kept constant. Fig. 3(a) shows percentage removal of Cr(VI) by PVA-Ag₂Te-Chitosan vs chitosan. It was observed that the percentage removal of Cr(VI) was high at low pH. The maximum percentage removal of Cr(VI) from the solution was discovered to be 82 % at a pH of 2 and 51 % at a pH of 2 for pure chitosan. The effect of contact time was

studied using the optimum pH of 2. Fig. 3(b) shows that the optimum time was found to be 60 min for pure chitosan with a percentage removal of 65 % and 120 min for PVA-Ag₂Te-Chitosan with a percentage removal of 79 %.

The effect of initial concentration is represented by Fig. 3(c). It was noted that at a lower concentration of 5 mg/L, a highest percent removals of Cr(VI) were discovered. The highest percent removal of Cr(VI) by pure Chitosan was found to be 52 % and 79 % by the PVA-Ag₂Te-Chitosan. When the concentration of chromium was increased to 90 mg/L, a decrease in the percent removal was observed. This is due to the fact that at higher concentrations of Cr(VI) in the solution, the available sites for the adsorption process become saturated and lead to blockage of pores for adsorption to take place.

3.2.2. Adsorption isotherms

Langmuir and Freundlich adsorption isotherms, which describe the interactions between the adsorbent and the adsorbate, were used to fit the data to explain the removal mechanism. The data for the Langmuir and Freundlich isotherms were calculated using (Equation (3)) and (Equation (4)), respectively. The Langmuir and Freundlich parameters for the adsorption of Cr(VI) ions by the 4 mL of PVA-Ag₂Te-chitosan as

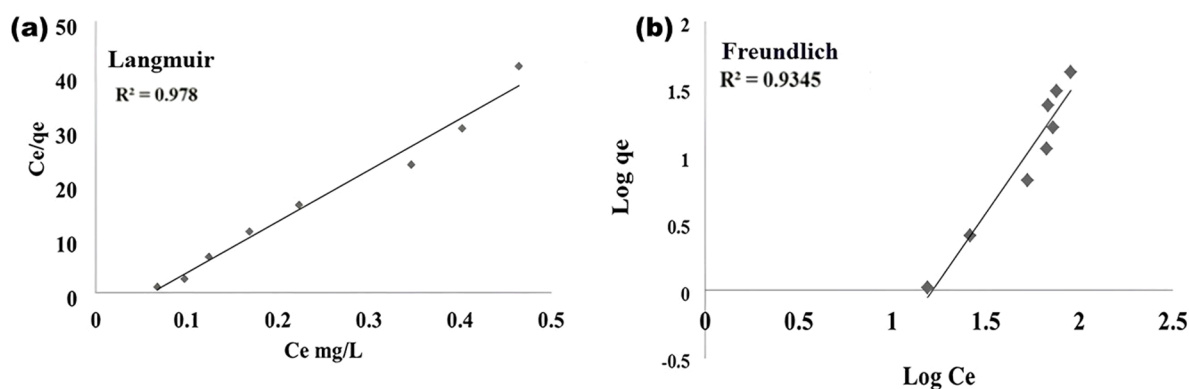
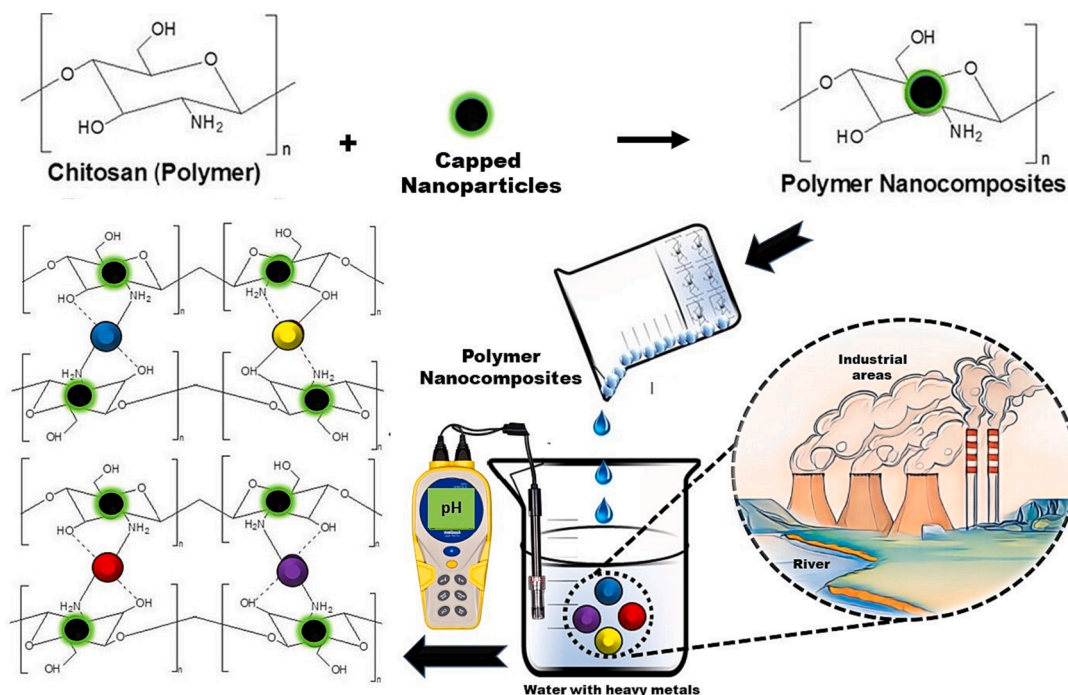


Fig. 4. Adsorption isotherms of PVA-Ag₂Te-Chitosan fitted to the Langmuir model (a) and Freundlich model (b).



Scheme 1. The mechanism of the formation of nanocomposites and the adsorption of heavy metal from wastewater using chitosan based nanocomposites.

an adsorbent are shown in Table 1. The correlation coefficient (R^2) value for the Freundlich model was 0.935 for PVA-Ag₂Te-Chitosan. The Freundlich model correlation coefficients (R^2) is less than that of the Langmuir model which is 0.978 for PVA-Ag₂Te-Chitosan. The maximum Langmuir monolayer adsorption capacity ($q_{e(cal)}$) was 97.087 mg/g for PVA-Ag₂Te-chitosan. This values was closer to the experimental adsorption capacity ($q_{e(exp)}$) 89.852 mg/g for PVA-Ag₂Te-chitosan. The K_L term of the Langmuir isotherm was less than 1 (0.160 Lmg^{-1}) for PVA-Ag₂Te-chitosan. The closeness of the experimental adsorption capacity ($q_{e(exp)}$) to the calculated adsorption capacity ($q_{e(cal)}$) and the higher correlation coefficients (R^2) for the Langmuir model led to the conclusion that the uptake mechanism followed a monolayer process. Favourable and unfavourable adsorption process between Cr and PVA-Ag₂Te-chitosan is predicted by the R_L value with a magnitude of 0.065. The results obtained showed a favourable adsorption process for this adsorbent as the R_L value was less than 1. The equilibrium data were matched to the Langmuir and Freundlich models, which are presented in Fig. 4 below.

3.2.3. Mechanism of heavy metal removal

The adsorption mechanism of metal ions involving chitosan and PVA-Ag₂Te-Chitosan nanocomposites has been extensively studied lately. It has been reported that metal ion complexes are formed as a consequence of an interaction between the metal ion, chitosan and its nanocomposites functional groups such as amino ($-\text{NH}_2$) and the hydroxyl ($-\text{OH}$) groups. Metal chelation occurs through the coordination of the chitosan and their corresponding nanocomposites with the metal cations. This may occur due to the lone pair of electrons that is present in each of the amino and hydroxyl groups that can be shared with metal cations. The adsorption of heavy metals also depends on the surface area and pore structure of the adsorbent [18,19]. When the PVA-Ag₂Te-Chitosan in Scheme 1 was dispersed in the Cr(VI) ions solution, an interaction between chitosan and the nanoparticles in the adsorption of Cr(VI) from aqueous solution occurred. The chitosan's functional groups ($-\text{NH}_2$ and $-\text{OH}$) coordinated with the Cr(VI) ions while the metal ions accept electron pairs from the amino and hydroxyl groups of chitosan and act as a Lewis acid [19,20].

4. Conclusion

The synthesis of PVA-Ag₂Te nanoparticles and PVA-Ag₂Te-chitosan nanocomposites for the effective removal of Cr(VI) ions from aqueous solutions is successfully reported. The absorption spectrum of the capped nanoparticles was blue shifted in comparison with the uncapped Ag₂Te nanoparticles. The TEM images revealed the average particles sizes that were corresponding to the crystalline sizes that were calculated from the Debye Scherrer formular. The optimum pH was found to be 2 and the removal efficiency was found to be dependent on the contact time and initial Cr(VI) ions concentration. PVA-Ag₂Te-chitosan nanocomposite disclosed the better percentage removal of Cr(VI) ion from wastewater compared to the pure chitosan solution. The adsorption isotherm data fitted the Langmuir model and the uptake mechanism followed a monolayer adsorption process. The obtained results confirmed that the polymer nanocomposites is a promising candidate as

a new generation adsorbent due to the high percentage removal of Cr (VI) ions than the pure chitosan.

CRedit authorship contribution statement

O. Sentse: Investigation, Formal analysis, Writing - original draft. **T. Xaba:** Supervision, Conceptualization, Investigation, Methodology, Project administration, Writing - review & editing. **N.D. Shooto:** Validation, Investigation, Writing - review & editing. **V.E Pakade:** Investigation, Supervision, Conceptualization, Writing - original draft. **W. Omwoyo:** Investigation, Supervision, Conceptualization, Writing - original draft.

Declaration of Competing Interest

The authors declare that they have no known competing financial interests or personal relationships that could have appeared to influence the work reported in this paper.

Data availability

Data will be made available on request.

Acknowledgements

The authors would like to acknowledge the Vaal University of Technology and National Research Foundation (TTK13071722088: "Thuthuka Grant Holder") for funding this project.

References

- [1] Q. Wang, J. Song, M. Sui, *Energy Procedia*. 5 (2011) 1104.
- [2] T. Xaba, J. Magagula, O.B. Nchoe, *Materials Letters* 229 (2018) 331.
- [3] D.P. Mungasavalli, T. Viraraghavan, Y.-C. Jin, *Colloids Surf A Physicochem Eng Asp.* 301 (2007) 214.
- [4] A. Bhatnagar, M. Sillanpa, *Chem Eng J.* 157 (2010) 277.
- [5] M.I. Skiba, A. Pivovarov, V. Vorobyova, *Chem. Chem. Technol.* 14 (2020) 47.
- [6] A.K. Samal, T. Pradeep, *J. Phys. Chem. C.* 113 (2009) 13539.
- [7] N. Kumar, S.S. Rayab, J.C. Ngila, *New J. Chem.* 41 (2017) 14618.
- [8] Y. Chang, J. Guo, Y.-Q. Tang, Y.-X. Zhang, J. Feng, Z.-H. Ge, *Cryst Eng Comm* 21 (2019) 1718.
- [9] M.I. Skiba, V.I. Vorobyova, I.V. Kosogina, *Journal of Chemistry* 2020 (2020) 5380950.
- [10] M. Nawaz, Z. Wahab, Z.U. Rehman, A. Bahader, M.I. Khan, I. Uddin, F.S. Gul, M. A. Bajaber, *Polym. Bull.* 80 (2023) 7545.
- [11] T. Xaba, *Green Processing and Synthesis.* 10 (2021) 374.
- [12] O.S. Oluwafemi, N. Revaprasadu, *Mater. Res. Soc. Symp. Proc.* 1138 (2009) 12.
- [13] N. Kumar, S.S. Ray, J.C. Ngila, *New J. Chem.* 41 (2017) 14618.
- [14] A.I. Shanmugapriya, A. Srividhya, R. Ramya, P.N. Sudha, *International Journal of Environmental Sciences.* 1 (2001) 2086.
- [15] A.A. Ebnalwaled, M.H. Essai, B.M. Hasaneen, H.E. Mansour, *Journal of Materials Science: Materials in Electronics* 28 (2017) 1958.
- [16] T. Xaba, M.J. Moloto, M. Al-Shakban, M.A. Malik, P. O'Brien, *Materials Science in Semiconductor Processing* 71 (2017) 109.
- [17] V.E. Pakade, C. Mareni, T.D. Ntuli, T.N. Tavengwa, *South African Journal of Chemistry.* 69 (2016) 180.
- [18] B. Kuchta, L. Firllej, G. Maurin, *J. Mol. Model.* 11 (2005) 293.
- [19] T. Xaba, M.J. Moloto, O. Nchoe, Z. Nate, N. Moloto, *Chalcogenide Letters* 11 (2017) 337.
- [20] E.D. Azzam, G. Eshaq, A.M. Rabie, A.A. Bakr, A.A. Abdelaai, E.E. Metwally, S. M. Tawfik, *International Journal of Biological Macromolecules.* 89 (2016) 507.